Am. J. Hum. Genet. 66:1504–1515, 2000

Mutation Analysis and Embryonic Expression of the *HLXB9* Currarino Syndrome Gene

D. M. Hagan,[1,*] A. J. Ross,[1,*] T. Strachan,[1] S. A. Lynch,[1] V. Ruiz-Perez,[1] Y. M. Wang,[1] P. Scambler,[2] E. Custard,[2] W. Reardon,[3] S. Hassan,[2] M. Muenke,[8] P. Nixon,[2] C. Papapetrou,[2] R. M. Winter,[3] Y. Edwards,[4] K. Morrison,[4] M. Barrow,[9] M. P. Cordier-Alex,[10] P. Correia,[11] P. A. Galvin-Parton,[12] S. Gaskill,[13] K. J. Gaskin,[14] S. Garcia-Minaur,[15] R. Gereige,[16] R. Hayward,[5] T. Homfray,[7] C. McKeown,[17] V. Murday,[7] H. Plauchu,[10] N. Shannon,[18] L. Spitz,[6] and S. Lindsay[1]

[1]Human Genetics Unit, School of Biochemistry and Genetics, University of Newcastle upon Tyne, Newcastle upon Tyne; [2]Molecular Medicine Unit and [3]Department of Clinical Genetics and Fetal Medicine, Institute of Child Health, [4]MRC Human Biochemical Genetics Unit, University College, [5]Department of Neurosurgery and [6]Nuffield Department of Surgery, Great Ormond Street Hospital for Children, and [7]Department of Medical Genetics, St. Georges Hospital Medical School, London; [8]Medical Genetics Branch, National Human Genome Research Institute, Bethesda; [9]Department of Clinical Genetics, Leicester Royal Infirmary, Leicester; [10]Hopital Hotel Dieu, Lyon; [11]IFF-Fiocruz, Rio de Janeiro; [12]Department of Pediatrics, State University of New York at Stony Brook, Stony Brook; [13]Medical Drive, San Antonio; [14]Royal Alexandra Hospital for Sick Children, Camperdown, New South Wales, Australia; [15]Clinica Materno-Infantil, Hospital de Cruces, Barakaldo, Spain; [16]All Children's Hospital, St. Petersburg, FL; [17]Clinical Genetics Unit, Birmingham Women's Hospital, Birmingham, United Kingdom; and [18]Centre for Human Genetics, Sheffield

The *HLXB9* homeobox gene was recently identified as a locus for autosomal dominant Currarino syndrome, also known as hereditary sacral agenesis (HSA). This gene specifies a 403–amino acid protein containing a homeodomain preceded by a very highly conserved 82–amino acid domain of unknown function; the remainder of the protein is not well conserved. Here we report an extensive mutation survey that has identified mutations in the *HLXB9* gene in 20 of 21 patients tested with familial Currarino syndrome. Mutations were also detected in two of seven sporadic Currarino syndrome patients; the remainder could be explained by undetected mosaicism for an *HLXB9* mutation or by genetic heterogeneity in the sporadic patients. Of the mutations identified in the 22 index patients, 19 were intragenic and included 11 mutations that could lead to the introduction of a premature termination codon. The other eight mutations were missense mutations that were significantly clustered in the homeodomain, resulting, in each patient, in nonconservative substitution of a highly conserved amino acid. All of the intragenic mutations were associated with comparable phenotypes. The only genotype-phenotype correlation appeared to be the occurrence of developmental delay in the case of three patients with microdeletions. *HLXB9* expression was analyzed during early human development in a period spanning Carnegie stages 12–21. Signal was detected in the basal plate of the spinal cord and hindbrain and in the pharynx, esophagus, stomach, and pancreas. Significant spatial and temporal expression differences were evident when compared with expression of the mouse *Hlxb9* gene, which may partly explain the significant human-mouse differences in mutant phenotype.

Introduction

The combination of partial absence of the sacrum, anorectal anomalies, and a presacral mass (anterior meningocoele or teratoma) constitutes Currarino syndrome, also known as "Currarino triad" (MIM 176450) (Currarino et al. 1981). Radiography of patients reveals preservation of the first sacral vertebra with a hemisacrum (sickle-shaped) remnant of sacral vertebrae 2–5 (S2–S5), either to the right or left. The anorectal abnormalities include imperforate anus, ectopic anal position, and a variety of inappropriate connections, either to the spinal cord or to the urogenital system. Considerable intrafamilial variation in expressivity is seen, including presentation in the neonate with acute bowel obstruction secondary to an imperforate anus, a history of chronic constipation from early childhood, and, at the mild end, asymptomatic individuals with sacral abnormalities.

The malformations seen in Currarino syndrome are in tissues that have their embryological origin in the tail bud and may reflect disturbances of secondary neurulation, a process that occurs during early development

Received November 16, 1999; accepted for publication February 21, 2000; electronically published April 4, 2000.

Address for correspondence and reprints: Drs. T. Strachan and S. Lindsay, Human Molecular Genetics Unit, School of Biochemistry and Genetics, Ridley Building, Claremont Place, Newcastle upon Tyne NE1 7RU, United Kingdom. E-mail: s.lindsay@newcastle.ac.uk or tom.strachan@ncl.ac.uk

* These authors contributed equally to this work.

0002-9297/2000/6605-0005$02.00

(Pang 1993; Lynch et al. 1995). In the human tail bud, the neural tube, notochord, somites, and hindgut all arise from a mass of pluripotential cells in the period commencing at Carnegie stage 12 (CS12 = 26 postovulatory d [POD]) (O'Rahilly and Muller 1987). A primary notochordal defect in the tail bud leading to its nonformation or mispositioning has been proposed as an explanation for the pathogenesis in Currarino syndrome (Currarino et al. 1981; Lynch et al. 1995).

We have mapped the locus for autosomal dominant Currarino syndrome, also called "hereditary sacral agenesis" (HSA), to chromosome 7q36 (Lynch et al. 1995). We recently reported elsewhere that patients with HSA have mutations in the *HLXB9* gene (Ross et al. 1998), a homeobox gene (formerly called *HB9*), which was first identified because of its expression in pancreatic and lymphoid tissues (Harrison et al. 1994). *HLXB9* has three exons and encodes a protein of 403 amino acids with three significant features (fig. 1*A*): a polyalanine repeat region which shows length polymorphism; a homeodomain encoded by exons 2 and 3 (see Harrison et al. 1994) and conserved among *HLXB9* homologues but not among other homeobox genes (with the exception of *Mnr2*—see fig. 1*B*); and a highly conserved region of 82 amino acids upstream of the homeodomain (Harrison et al. 1994; Saha et al. 1997; A. J. Ross, T. Strachan, and S. Lindsay, unpublished data).

Two *Hlxb9−/−* strains of knockout mice have been described, but both of their phenotypes are rather different from that shown by human patients. Heterozygotes have no discernible phenotype, but the two homozygous knockouts show similar abnormalities of pancreatic (Harrison et al. 1999; Li et al. 1999) and motor-neuron development (Arber et al. 1999; Thaler et al. 1999), neither of which is evident in patients with *HLXB9* mutations. In addition, neither of the mouse mutants had any detectable disruption of sacral or hindgut development.

In the present study, we report *HLXB9* mutation analyses in 28 patients with familial or sporadic Currarino syndrome. Mutations were detected in 20 of 21 patients with familial Currarino syndrome and in 2 of 7 patients with sporadic Currarino syndrome. Similar phenotypes were attributable to a variety of different classes of intragenic mutation, consistent with pathogenesis caused by loss of function. Missense mutations were identified in a total of eight unrelated index patients with Currarino syndrome. All of the missense mutations mapped to the homeobox, and none mapped to the highly conserved domain preceding it. Screening of a group of mainly sporadic patients with related or partial phenotypes or additional atypical features failed to detect *HLXB9* mutations. We also report an extended study of *HLXB9* embryonic expression, which has revealed significant human-mouse differences in both spatial and temporal expression patterns. We discuss these findings in the light of the highly significant human-mouse differences in the associated phenotypes.

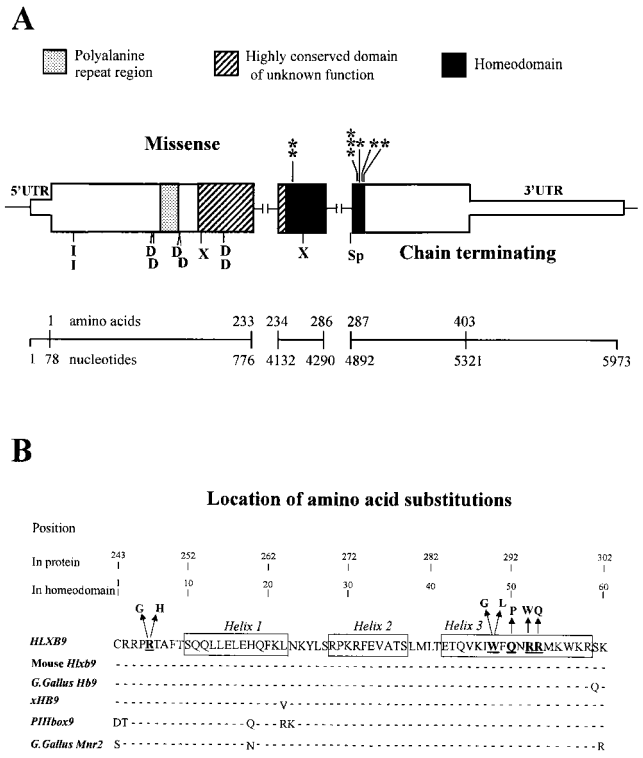

Figure 1 Location of intragenic *HLXB9* mutations. *A,* Spectrum of missense and chain-terminating mutations. The three exons of *HLXB9* gene are denoted by rectangular boxes with the coding sequences emphasized by wider boxing than that used for the flanking 5′ and 3′ UTR sequences. Missense mutations are denoted by asterisks (*) above the exons. The locations of different classes of chain-terminating mutations are indicated by lettering below the gene, as follows: I = frameshifting insertions; D = frameshifting deletions; X = nonsense mutations; Sp = splice-site mutation. *B,* Amino acid substitutions resulting from missense mutations. Substituted amino acids are indicated by bold, underlined letters, and the derived mutant residues are shown in bold above the arrowheads. The W290G mutation was found in two unrelated patients (35 and 37; see table 1). Reference sequences were derived as follows: *HLXB9*: Harrison et al. (1994), corrected for codon 264 from our unpublished data; mouse *Hlxb9* (formerly *Hb9*): Arber et al. (1999) and Thaler et al. (1999); chick (*Gallus Gallus*) *HB9*: Pfaff et al. (1996); *Xenopus* (*xHB9*): Saha et al. (1997); sea urchin (*PIHbox9*): Bellomonte et al. (1998); chick *Mnr2*: Tanabe et al. (1998). Dashes denote identity. As can be seen from the figure, the homeodomain of *Mnr2* is highly homologous to that of *HLXB9,* but, outside the homeodomain, the proteins are not related. *Mnr2* is expressed in dividing neuroblasts and plays a major role in motor neuron specification in the chick (Tanabe et al. 1998).

Patients and Methods

Patients

Ethical permission for the study was given by the Joint Ethics Committee of the Newcastle Health Authority.

Patients showing Currarino syndrome (including three with developmental delay) were investigated. The clinical details of families 1, 2, 14, 16, 19, 20, 23, 27, and 29 have been reported elsewhere (Cavero Vargas et al. 1992, Hardwick et al. 1992; Gaskill and Marlin 1996; Ross et al. 1998 and references therein). DNA samples from 28 index patients and their families were prepared and analyzed. The phenotypes of the patients in whom we found a mutation are given in table 1. The family in which we did not identify an *HLXB9* mutation (family 24) initially presented following the birth of a child with Currarino syndrome. Features noted included anal atresia, a partial sacral agenesis, and a presacral mass. As children, the child's father and paternal uncle had surgery to remove teratomas from the intestine and mediastinum, respectively. Sacral X-rays were not available from either.

DNA samples from a further 32 patients with partial, atypical, or related phenotypes were also investigated. They comprised patients with anorectal malformations (n = 9), with sacral agenesis (n = 12—these patients did not have hemisacrum, and some had additional malformations), with sacroccocygeal teratomas (n = 2), and with spina bifida occulta (n = 9).

Table 1

***HLXB9* Mutations Identified in the Study and Associated Phenotypes**[a]

Mutation Class	Mutation Position	Nucleotide Change	Amino Acid Change	Clinical Phenotype[b]	Family or Patient No.
Missense	Homeobox	C→G, nt 4171	R247G	Hemisacrum, ARM, presacral mass, perianal abcess	3
		G→A, nt 4172	R247H	Hemisacrum, ARM, presacral mass	13
		T→G, nt 4900	W290G	Hemisacrum, ARM, presacral mass, rectovaginal fistula, neurogenic bladder	35[c]
		T→G, nt 4900	W290G	Hemisacrum, ARM, presacral mass, tethered cord	37[c]
		G→T, nt 4901	W290L	Hemisacrum, ARM, presacral mass	30
		A→C, nt 4907	Q292P	Hemisacrum, ARM, presacral mass,	5
		C→T, nt 4912	R294W	Hemisacrum, ARM, presacral mass, vesico-ureteric reflux	38
		G→A, nt 4916	R295Q	Hemisacrum, ARM presacral mass, renal malformation	14
Splice Site	Homeobox	A→G, nt 4889	NA	Hemisacrum, ARM, presacral mass, nonpenetrance[d]	16
Frameshift	Exon 1	Ins C, nt 125-30	NA	Hemisacrum, ARM, presacral mass, neurogenic bladder, nonpenetrance	20
		Ins C, nt 125-30	NA	Hemisacrum, ARM, presacral mass (detected antenatally)	23
		Del G, nt 408-13	NA	Hemisacrum, ARM, presacral mass	26
		Del C, nt 414-17	NA	Hemisacrum, ARM, presacral mass	19
		Del 14nt, nt 483-96	NA	Hemisacrum, ARM, presacral mass	27
		Del G, nt 486-90	NA	Hemisacrum, ARM, presacral mass, tethered cord	36
		Del A, nt 652-53	NA	Hemisacrum, ARM	2
		Del A, nt 652-53	NA	Hemisacrum, ARM, presacral mass	33
Nonsense	Exon 1	C→A, nt 575	Y166X	Sporadic, hemisacrum, ARM, presacral mass, tethered cord	29
	Homeobox	C→T, nt 4213	Q261X	Hemisacrum, ARM, presacral mass, bicornuate uterus[e]	1
Microdeletion	Hemizygous deletion of *HLXB9*	NA	NA	Hemisacrum, ARM, developmental delay	6
		NA	NA	Absent sacrum/short stature/single central incisor, developmental delay	32
		NA	NA	Sporadic, hemisacrum, ARM, presacral mass, tethered cord, developmental delay	34

[a] In addition to patient-specific mutations, polymorphisms were also detected: del C in a run of 4Cs at positions −519 to −522 (frequency of del C allele = .1); C/G at –293 bp upstream of ATG (frequency of G allele = .175); A/G 92 bp into intron 2 from the 5′ end (frequency of G allele = .09); T/C 131 bp upstream of exon 3 (frequency of C allele = .44).

[b] All patients are familial except, as indicated, sporadic patients 29 and 34. The clinical features documented in the familial patients are descriptive of the range of features seen collectively (i.e., not all features were present in all individuals.) ARM = anorectal malformation.

[c] Although these two families have the same mutation, haplotype analysis using very closely linked proximal and distal markers strongly suggests that they arose independently (see Results).

[d] Nonpenetrance in at least one family member.

[e] One death in affected from brain tumor; possible malignant change in known teratoma.

Mutation Analysis

Nine overlapping oligonucleotide primer pairs were designed to amplify the *HLXB9* coding region by PCR (fig. 1*A*). They were four primer pairs in exon 1 (1*A*–1*D*), one in exon 2, and four in exon 3 (3*A*–3*D*). The precise positions of the primer pairs are shown in the study by Ross et al. (1998). Their sequences are given in the 5′→3′ direction in the accompanying table (Electronic-Database Information Section). Primers were also designed to amplify two segments of intron 2 (intron 2 5′ and intron 2 3′) and to span a putative promoter region of the gene. Features within the putative promoter region, which extends ~750 bp upstream of the presumed ATG start codon, include a potential CAAT box (121–125 bp upstream of the ATG) as well as 12 GC boxes (SP1 binding sites). As with other CpG island genes, there is no TATA box. The putative promoter was amplified using three primer pairs—PRA, PRB, and PRC. The sequences of these primers and the intronic primers are also given in the accompanying table (Electronic-Database Information).

PCR reactions and SSCP gel analysis were carried out as described elsewhere (Ross et al. 1998). All of the PCR mixes were supplemented with 2 M Betaine, with the exception of that for primer pair 1D, which was supplemented with 7.5% dimethyl sulfoxide. When a reproducible alteration was identified by SSCP gel analysis, the corresponding PCR fragment was cloned and sequenced as described elsewhere (Ross et al. 1998), to define the nature of the sequence change.

Microsatellite Analyses

Microsatellite analyses were carried out as described by Ross et al. (1998). The *HLXB9* gene was related to marker order by the following sequence: centromere-D7S637-EN2-D7S550-CGR13-D7S559-HLXB9-CGR16-D7S2423-D7S594-telomere (Ross et al. 1998; Heus et al. 1999).

In Situ Hybridization on Human Embryo Sections

Collection and use of human embryos was carried out with ethical permission from the Joint Ethics Committee of the Newcastle Health Authority and with the appropriate signed consents. Embryos were collected, following either surgically or medically induced termination of pregnancy (Bullen et al. 1998) and were staged by microscopic examination. Their fixation and processing for in situ hybridization are as described by Ross et al. (1998), as are the *HLXB9* sense and antisense probes and the in situ hybridization procedures. At all stages, adjacent sections were hybridized with antisense *HLXB9* or sense *HLXB9* probes. No signal was detected with the control sense probes (data not shown).

Results

Mutation Analyses

Patients were considered to have Currarino syndrome if they showed all three major features of the disorder—partial sacral agenesis (hemisacrum and not involving the first sacral vertebra [S1]), constipation or anorectal malformation, and presacral mass. In all cases (except family 2), at least one family member showed all three major features. Family 2 refused further clinical investigations, so the presence of a presacral mass could not be confirmed. In another family (33), however, the same mutation caused Currarino syndrome. The phenotypes found in the 22 families and sporadic patients in whom we detected a mutation are given in table 1. The intragenic mutations were not found in a panel of 258 control chromosomes. In three of the patients (6, 32, and 34) pathogenesis was due to a microdeletion that encompassed the *HLXB9* gene, as revealed by microsatellite typing using eight markers in the D7S637–D7S594 interval (see Methods; data not shown). Two of these patients, 6 and 34, had Currarino syndrome and developmental delay. In addition to these features, the third patient, 32, had a single maxillary incisor, a feature associated with holoprosencephaly.

The remaining 19 index patients (patients from 18 families and one sporadic patient) revealed intragenic mutations (see table 1). They consisted of eight frameshifting insertions/deletions, two nonsense mutations (one in exon 1 and one leading to a premature stop codon in the homeobox), a splice-site mutation (at the intron 2 splice acceptor), and eight missense mutations. Of the total of 19 intragenic mutations, there were 17 different mutations: families 2 and 33 have identical single-base deletions, whereas families 35 and 37 exhibited the same missense mutation. Families 2 and 33 both come from the same city in the north of England, and, although we have not been able to trace a link between them, it is likely that they are related. Families 35 and 37, however, were shown by microsatellite analyses to be carrying the mutation on chromosomes with quite different flanking markers. The haplotypes for the sequence of markers (cen-EN2-D7S550 -CGR13-D7S559-CGR16-D7S2423-D7S594-tel) were unambiguously derived as follows: 3-4-5-8-4-4-3 in family 35 and 3-2-1-5-3-2-2 in family 37 (data not shown). Because the marker *D7S559* is 180 kb proximal to *HLXB9* and *CGR16* is only 110 kb distal to *HLXB9* (Heus et al. 1999), these data support the view that the same missense mutation has occurred independently in families 35 and 37.

The position of the intragenic mutations is summarized in figure 1*A*. It is remarkable that all eight missense

mutations cluster in the homeobox even though the upstream sequence specifies a very highly conserved domain of 82 amino acids of unknown function. Each of the missense mutations result in nonconservative amino acid substitution in the homeodomain, involving amino acids in the third helix in five patients and two different substitutions of an arginine residue at the fifth amino acid position of the N-terminal arm (fig. 1*A*, *B*). In each patient, the substituted amino acid is one that has been highly conserved in evolution, being present in *HLXB9* orthologues in mouse, chick, *Xenopus,* and sea urchin and also in the homeodomain of the related chick *Mnr2* gene (fig. 1*B*).

In addition to patients with Currarino syndrome, we also screened a further 32 patients with overlapping, atypical, or related phenotypes. They consisted of patients with anorectal malformations ($n = 9$), sacral agenesis ($n = 12$; these patients did not have hemisacrum and some had additional malformations), sacroccocygeal teratomas ($n = 2$), and spina bifida occulta ($n = 9$); however, no *HLXB9* mutations were detected.

Embryonic Expression of HLXB9

As detailed in the Introduction, there are substantial human-mouse differences in mutant phenotypes associated with loss-of-function *HLXB9/Hlxb9* mutations. Although patients with Currarino syndrome are heterozygotes and the mutant-mouse phenotype is observed only in homozygotes, parallel examples are known with comparable phenotypes in human heterozygotes and mouse homozygotes (e.g., mutant sonic hedgehog phenotypes [reviewed in Ming and Muenke 1998]). This may suggest that there are other differences in the expression or function of *HLXB9/Hlxb9* that are significant for understanding the human disease. Although detailed embryonic-expression studies have only recently been initiated to study human genes, human-mouse differences have already been identified in embryonic expression for a variety of human disease genes and developmental control genes (see Fougerousse et al. 2000 and references therein).

We elsewhere reported a study of *HLXB9* expression in embryonic sacral development (Ross et al. 1998). In the current study, we carried out detailed, embryowide analyses of *HLXB9* expression. The malformations seen in Currarino syndrome are in tissues that have their embryological origin in the tail bud. The formation in the human tail bud of the definitive notochord, the hindgut, and caudal skeletal elements and the process of secondary neurulation occur in the period commencing at CS12 (O'Rahilly and Muller 1987). We have therefore carried out expression analyses to cover the period from CS12 to CS21, corresponding to 26–52 POD.

HLXB9 expression was detected in the neural tube at CS12 (26 POD), and by CS14 (31 POD) it was evident in the anterior horns (where motor neurons develop) and in the adjacent subventricular region. The population of cells in the anterior horns was detectable along the length of the neural tube (fig. 2*b*) and throughout the developmental period studied. The signal in the subventricular zone, however, gradually disappeared in a rostral to caudal direction: at CS19 it was not detectable at the level of the esophagus but was still present in the sacral region, where, in turn, the signal was not detectable by CS21 (fig. 2*d–f* and data not shown). Expression also extended rostrally into the hindbrain (the pyramidal tract region of the future medulla oblongata [fig. 2*b*]).

By CS15 (33 POD) clear expression of *HLXB9* was detected in the pharynx (data not shown) and the esophagus (fig. 3*b*), which persisted through all the developmental stages examined (see, e.g., fig. 2*b*). Foregut expression extended caudally as far as the developing stomach (fig. 3*d*) until CS17, after which time it was no longer detectable. In addition, at CS15, *HLXB9* was clearly detected in the dorsal pancreatic bud (data not shown), which arises from the most caudal region of the foregut. From CS17 (41 POD) onward, pancreatic expression of *HLXB9* was seen in both the dorsal bud and the now discernible ventral bud of the developing pancreas (fig. 3*f*). Expression appeared to be of similar intensity in both dorsal and ventral pancreatic buds, and *HLXB9* remained strongly expressed at CS19 and CS21 (fig. 3*h* and data not shown). No expression was seen in the midgut (fig. 2*b*) or hindgut throughout the embryonic period studied (data not shown). We did not detect expression in the notochord (in the sacral region or any other region; data not shown), and in the period studied the only sacral region where signal could be detected was in the spinal cord (see above and fig. 3*h*).

Discussion

HLXB9 *Mutations Account for the Pathogenesis of the Vast Majority of Patients with Familial Currarino Syndrome But Are Evident Only in a Proportion of Sporadic Patients*

We identified *HLXB9* mutations in 20 of 21 families and two of seven sporadic patients with Currarino syndrome, giving an aggregate 79% detection rate for independent mutations resulting in Currarino syndrome. We detected three instances of new mutations: two occurred in sporadic patients (29 and 34); the other one in an individual who subsequently transmitted the disease (3). The parent of origin was maternal in one patient, paternal in the second, and we were unable to determine it in the third patient. The *HLXB9* gene coding and putative promoter regions were sequenced in

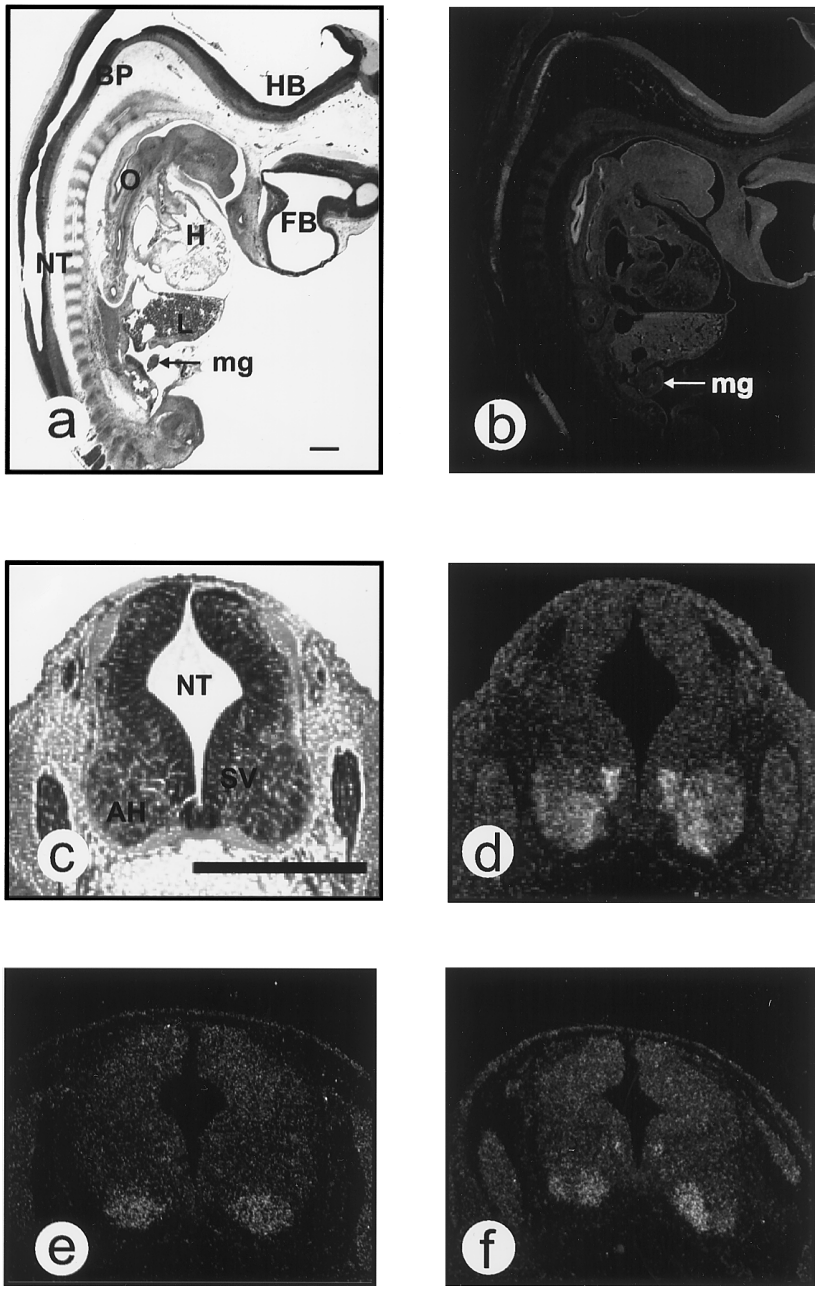

Figure 2 Basal plate expression of *HLXB9*. *A,* Bright field microscopy of a CS18 (44 POD) sagittal section stained with hematoxylin and eosin. *B,* Dark field microscopy of an adjacent section following in situ hybridization of antisense *HLXB9* probe. Expression can be seen throughout the length of the spinal cord (where present in the section; indicated as NT) and into the hindbrain. Expression is also seen in the developing esophagus but is not detectable in the midgut (*arrows*). *C,* High-power view of a transverse section of spinal cord in a CS17 (41 POD) embryo stained with hematoxylin and eosin and, *D,* corresponding dark-field view with expression clearly absent from the layer nearest the neural tube lumen (ventricular layer) and strongly detected in the subventricular and outer layers. *E* and *F,* Dark field views of expression in transverse sections of the spinal cord of a CS19 embryo at the level of the esophagus (*E*) or sacrum (*F*). At both levels, expression is clearly seen in the anterior horns, but by this stage expression is not detectable in the subventricular layer rostrally in the spinal cord (*E*) but is still detectable in more caudal regions (*F*). Adjacent sections in all patients were hybridized to sense *HLXB9* probe as a control. No specific signals were detected (data not shown). Bar = 500 μm. Indicated tissues are AH, anterior horn; BP, basal plate; FB, forebrain; HB, hindbrain; H, heart; L, liver; mg, midgut; NT, neural tube; O, (o)esophagus; and SV, subventricular layer.

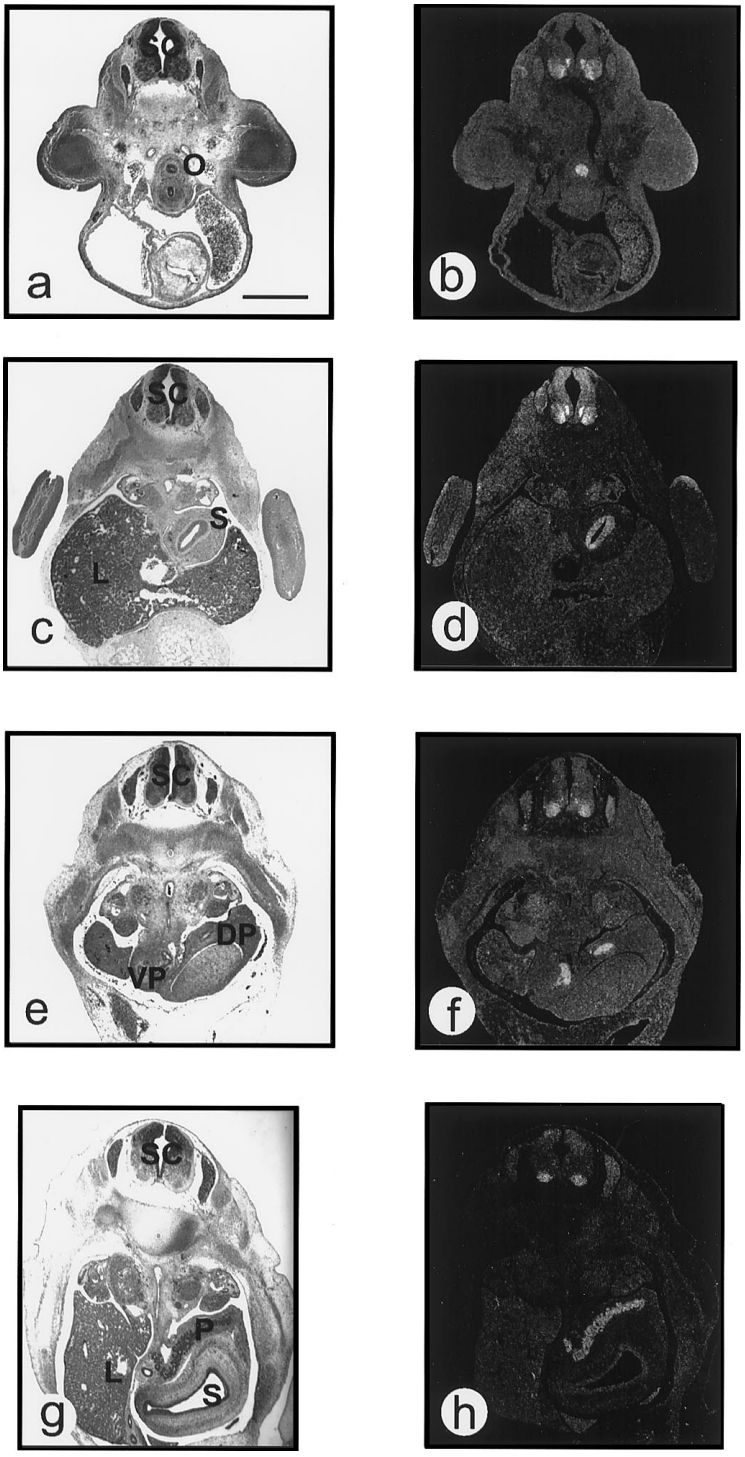

Figure 3 Expression of *HLXB9* in CS15 (*a–d*), CS17 (*e* and *f*), and CS19 (*g* and *h*) human embryos. The figure shows dark field photomicrographs of antisense *HLXB9* probe following in situ hybridization to transverse sections of CS15 (*b* and *d*), CS17 (*f*), and CS19 (*h*) embryos. Bright field microscopy of adjacent sections (*a, c, e,* and *g,* respectively) stained with hematoxylin and eosin are shown for orientation. Adjacent sections in each patient were hybridized to sense *HLXB9* probe as a control. No specific signals were detected (data not shown). At all three stages (CS15, CS17, and CS19), signal is clearly detected in the anterior horns of the spinal cord (*b, d, f, h*). At CS15, expression is detected in the developing esophagus (*b*) and stomach (*d*). At CS17, expression is detected in both the dorsal and ventral pancreas (*f*) and is still detectable in the pancreas at CS19 (*h*). At CS19, expression is not detected in the stomach (*h*). Bar = 500 μm. DP = dorsal pancreas; L = liver; O = (o)esophagus; P = pancreas; S = stomach; SC = spinal cord; VP = ventral pancreas.

five of the index patients with Currarino syndrome (one familial and four sporadic) in whom no mutation was detected by SSCP, but this did not reveal any mutations (data not shown). It remains possible that mutations elsewhere in the *HLXB9* gene may lead to the clinical phenotype, or, in the case of the sporadic patients, perhaps the mutation is not present in blood cells because of somatic mosaicism. Mutations leading to differential allele expression could be assessed using the intragenic exon 1 polymorphism specifying the variable-length polyalanine region, but, unfortunately, RNA samples were unavailable to us. We were also unable to obtain different tissue samples from the sporadic patients to test for somatic mosaicism.

The family in which we have not found a mutation in the *HLXB9* gene could indicate that there is genetic heterogeneity in familial Currarino syndrome. Linkage studies in this family are consistent with a locus on 7q36, however, although, because this is a small family, the LOD score is not significant (data not shown). The index patient in this family has all three features typical of Currarino syndrome, but the other two affected members of the family (her father and paternal uncle) have very atypical phenotypes (family 24; see Patients and Methods). It is, therefore, not clear whether the disorder is familial or the index patient is sporadic. Thus, although we cannot completely exclude the possibility of low-level heterogeneity, the mutation data presented here coupled with the fact that linkage analyses in all suitably large families are consistent with a single locus on 7q36 (Lynch et al. 1995; Vargas et al. 1998) strongly implicate *HLXB9* as the sole cause for familial Currarino syndrome.

HLXB9 mutations were detected in only a portion of sporadic patients with Currarino syndrome. Although mutations outside the coding and putative promoter regions and somatic mosaicism provide possible explanations, an alternative possibility is genetic heterogeneity. Possible candidate genes include genes known to be involved in the same pathways as *HLXB9*. *Isl1* and *Lim3,* like *Hlxb9,* are involved in motor neuron development (Pfaff et al. 1996), and, like *Hlxb9, Isl1* is also important in pancreas development (Harrison et al. 1999; Li et al. 1999). We used SSCP analyses to screen for mutations in the coding sequence of *ISL1* in the sporadic Currarino syndrome patients who do not have an *HLXB9* mutation, but no sequence changes were detected other than an already reported silent polymorphism at codon 168 (Riggs et al. 1995; A. J. Ross, T. Strachan, and S. Lindsay, unpublished data). At the time of this writing, the sequence of the human *LIM3* gene was unavailable; when this and the sequences of other interacting human genes become available, they too can be screened.

In contrast to patients with Currarino syndrome, *HLXB9* mutations were not detected in the group of 32 patients with atypical or partial or related phenotypes. Among them were nine patients with spina bifida occulta, a defect in which the vertebral arches, most commonly in the lumbar-sacral region, fail to fuse (Anderson 1975). This condition occurs sporadically and in families with neural tube defects and is, like Currarino syndrome, thought to be a defect of secondary neurulation (Pang 1993; Mclone and Dias 1994*a,* 1994*b*); however, patient-specific mutations were not evident in these patients.

Different Mutation Classes Produce Comparable Phenotypes, Most Likely as a Result of Haploinsufficiency, But Missense Mutations Are Significantly Clustered in the Homeobox

Our initial report described mutations that could result in premature introduction of a stop codon in *HLXB9* (Ross et al. 1998). The current study now provides a variety of disease-associated missense mutations. In addition, it provides further evidence that the phenotype is due to haploinsufficiency, because different mutation classes (7q36 microdeletions, missense mutations, nonsense mutations, frameshifting deletions, and splice-site mutations) all produce comparable phenotypes (table 1). The phenotypes in the patients with microdeletions not unexpectedly also showed developmental delay. In one patient , 32, there was also evidence of holoprosencephaly. FISH analyses using *SHH* cosmid probes have demonstrated that the *SHH* gene is also deleted in this patient (32; data not shown). There were no clear correlations between mutation type and severity of disease or incidence of specific clinical feature (sacral agenesis, anorectal malformation, constipation, anterior meningocoele, lipoma/teratoma, malignancy, perianal sepsis, spinal cord tethering [table 1 and data not shown]). Individual mutations were, however, frequently accompanied by variable expressivity in families with multiple affected individuals. About 1/3 presented as neonates or in early childhood requiring surgical intervention, whereas other symptomatic individuals were able to be managed conservatively, thus avoiding surgery (S. A. Lynch, unpublished observations). Many affected individuals were asymptomatic but usually had evidence of sacral abnormalities on X-ray, with the exception of two families where nonpenetrance was a feature (families 16 and 20) (table 1 and Ross et al. 1998).

All of the identified missense mutations result in substitution of a very highly conserved amino acid that appears from in vitro assays to be involved in the binding of the homeodomain to the target DNA motif TAAT (Kissinger et al. 1990; Gehring et al. 1994). Four of the substituted amino acids (W48, Q50, R52, and R53) are

in helix 3, the recognition helix. The fifth (R5) is one of the small number of residues in the N-terminal arm (otherwise largely involved in protein-protein interactions [Di Rocco et al. 1997]) that have also been shown to be important for binding to TAAT. The importance in vivo of these specific amino acid positions in the homeodomain has been underscored by parallel findings in other homeobox genes underlying human genetic disorders (see, e.g., Dattani et al. 1998; Villa et al. 1998; Swaroop et al. 1999).

It is striking that all missense mutations reported here are in the homeobox. Although we identified seven different missense mutations (fig. 1*A, B*), the identification of identical missense mutations in two unrelated families with entirely different marker haplotypes (35 and 37; see Results and table 1) strongly suggests eight independent missense mutations. To our knowledge, only two other *HLXB9* missense mutations have been identified in Currarino syndrome patients, and they too are located in the homeobox resulting in R295W and T248S substitutions (Belloni et al. 2000). Thus, 10/10 missense mutations map to the homeobox, although the sequence immediately upstream encodes a highly conserved 82–amino acid domain of unknown function. The size of this domain varies slightly in orthologues, principally as a result of length variation in a second polyalanine repeat region distinct from the polymorphic polyalanine tract. Outside this length variation, the *HLXB9* sequence shows >96%, 91%, and 80% identity to orthologues in mouse, chick, and *Xenopus,* respectively. Possibly, as with many other homeobox genes, the second highly conserved domain encoded by *HLXB9* could have a regulatory role and/or be involved in protein-protein associations. In this case, it is conceivable that amino acid substitutions in this domain could give rise to different clinical phenotypes.

HLXB9 *Expression in Early Human Embryos Shows Significant Differences When Compared with the Mouse Orthologue, But Neither Expression Pattern Is Easily Related to the Human Phenotype*

A primary notochordal defect in the tail bud leading to its nonformation or mispositioning has been proposed as an explanation for the pathogenesis in Currarino syndrome (Currarino et al. 1981; Lynch et al. 1995). The consistent inability to detect *HLXB9* expression in tail bud notochord from CS12 onward (data not shown), or in more anterior regions of the notochord (figs. 2 and 3), could conceivably reflect very low-level *HLXB9* expression that is undetectable by standard in situ hybridization techniques. It is also possible that significant expression occurs in notochordal/prenotochordal tissue at stages prior to CS12. In the mouse, very recent reports have described early notochordal expression for *Hlxb9*, both in the tail bud and more anteriorly, and this expression pattern can no longer be detected by E10, which corresponds approximately to CS12 (Harrison et al. 1999; Li et al. 1999). If *HLXB9* is expressed in the human notochord, therefore, it may be affecting very early notochord formation, and it could be downstream "effectors" that are active at the time of definitive notochord and vertebral formation.

HLXB9 expression was detected in developing human motor neurons (mostly postmitotic neurons in the anterior horn) throughout the length of the developing spinal cord, as well as in the basal plate of the hindbrain (fig. 2*b*). Although, in *Xenopus* and chick, *Hlxb9* expression is detected only in postmitotic motor neurons (Saha et al. 1997; Tanabe et al. 1998), the human and mouse orthologues appear to show some additional expression in motor-neuron progenitors. In mouse, the expression of *Hlxb9* in dividing motor-neuron progenitors is indicated by the presence of BrdU+/Hb9+ cells and Lim3+/Hb9+/Isl1- cells (Arber et al. 1999), and expression of human *HLXB9* in the subventricular zone (see fig. 2*d, f*) may suggest that, as it is in the mouse, *HLXB9* is also expressed in some cells at an earlier stage of the cell cycle than in the chick. The only direct spinal cord feature of Currarino syndrome is spinal cord tethering, but it is unclear whether or how this expression is related to the observed *HLXB9* expression patterns. In contrast to patients with Currarino syndrome, *Hlxb9* −/− knockout mice have motor-neuron abnormalities (Arber et al. 1999; Thaler et al. 1999), and in mouse, *Hlxb9* is required to consolidate and, possibly, maintain motor-neuron identity within the spinal cord. Its absence, in *Hlxb9*−/− knockout mice, leads to an increased number of V2 interneurons as well as abnormalities of motor-neuron projection. They, however, are not restricted to the sacral region but occur at all levels of the spinal cord examined (Arber et al. 1999; Thaler et al. 1999).

HLXB9 expression in the developing gut shows significant differences when compared to mouse *Hlxb9* expression. *HLXB9* is expressed in the developing foregut (the pharynx, esophagus, and, transiently, in the stomach; fig. 3*b, c*), but, despite detailed examination, no expression could be detected in either the midgut (fig. 2*b*) or the hindgut (data not shown). Patients in our series with *HLXB9* mutations do not manifest abnormalities in tissues deriving from the foregut, possibly as a result of functional compensation or lack of sensitivity in such tissues to 50% dosage, whereas hindgut is expected to be relevant to the human pathogenesis. In the embryonic period studied (CS12–CS21), there is major development of the hindgut, including the caudal extension of the urorectal septum that divides the cloaca into the anterior portion, containing the primitive urogenital

sinus, and the posterior anorectal canal. The urorectal septum reaches the cloacal membrane, which then ruptures to form the anus at CS18/CS19. Incorrect growth and positioning of the urorectal septum could lead to the anorectal malformations and abnormal bifurcations of the urogenital system seen in a proportion of patients with Currarino syndrome. In mouse, no expression of *Hlxb9* is reported in the hindgut at comparable embryonic stages. *Hlxb9* expression has been shown in the entire dorsal gut endoderm at very early stages (E8), which persists in both the foregut (esophagus and stomach) and also, unlike in humans, the midgut (Harrison et al. 1999; Li et al. 1999). It is known that there are considerable differences in the timing of human and rodent gut differentiation at later stages to the ones studied here: after ~8–10 wk of development in human and 13 embryonic d in mouse (Klein 1989; Kedinger 1994). Differences in gene-expression patterns at earlier stages could be important in establishing the later differences in the timing of morphological and differentiation events. Other studies have also shown differences in gene expression in gut development between human and mouse at early stages (e.g., Yamaguchi et al. 1999; Fougerousse et al. 2000; see also Lindsay et al. 1997).

Our expression study shows that *HLXB9* is expressed early in human pancreatic development, at the time before fusion of the dorsal and ventral buds. Expression is detected earlier in the dorsal bud compared to ventral bud, possibly because of the very small initial size of the latter. In mouse, *Hlxb9* expression is detectable in both dorsal and ventral pancreatic buds at E9.5, but its expression rapidly decreases, initially in the ventral bud, and is undetectable in both dorsal and ventral buds by E10.5/E11.5. At later stages, expression is again detected becoming progressively more restricted to the beta cells of the islets of Langerhans (Harrison et al. 1999; Li et al. 1999). This is unlike *HLXB9*, which in human continues to be expressed throughout the period studied with no obvious differences in intensity of expression between the dorsal and ventral buds after CS15. These differences in the timing of expression and relative intensities of expression between the dorsal and ventral buds may reflect underlying differences in the development of human and murine pancreas.

Although pancreatic malformations or malfunction have not been described in Currarino syndrome, pancreatic *HLXB9* expression is of interest given the association between maternal diabetes and caudal dysplasia (Kalter 1993) and the caudal malformations elicited in animals as a result of the teratogenic effects of insulin (reviewed by Alles and Sulik 1993). There is a wide spectrum of defects seen in caudal dysplasia, including abnormalities of the sacrum and hindgut (Pang 1993), but the possibility that *HLXB9* may be involved is raised by the reports of several patients with 7q36 deletions (Morichon-Delvallez 1993; Savage et al. 1997). It is interesting that neuronal abnormalities are part of the spectrum of caudal dysplasia, with motor nerves being more severely affected than sensory ones (Pang 1993). We are currently undertaking a mutation study of caudal dysplasia patients to assess the involvement of *HLXB9* in these disorders.

Acknowledgments

We would like to thank the families who agreed to take part in this study and the many clinicians who have generously provided us with patient samples. We are also grateful to Dr. Peter Heutink, for supplying information about markers CGR13 and CGR16 prior to publication; Mr. Ian Cross, for help with the analysis of the microdeletions; Dr. Harinder Gill, for additional clinical help; and Dr. Michele Kedinger, for helpful discussions on gut development. We would also like to thank the Medical Research Council, the Wellcome Trust, the Sir Jules Thorn Charitable Trust, Action Research, and the William Leech Charity, for their support.

Electronic-Database Information

Accession numbers and URLs for data in this article are as follows:

Department of Genetics, Hospital for Sick Children, University of Toronto, http://www.genet.sickkids.on.ca/chromosome7/ (for chromosome 7 map information)

Human Genetics Unit, School of Biochemistry and Genetics, University of Newcastle upon Tyne, http://www.ncl.ac.uk/human.genetics/hlxb9.html (for PCR-primer details)

Life Sciences Division, Oak Ridge National Laboratory, http://www.ornl.gov/hgmis/launchpad/chrom07.html (for chromosome 7 information)

Online Mendelian Inheritance in Man (OMIM), http://www.ncbi.nlm.nih.gov/Omim (for Currarino syndrome [MIM 176450])

References

Alles AJ, Sulik KK (1993) A review of caudal dysgenesis and its pathogenesis as illustrated in an animal model. Birth Defects 29:83–102

Anderson F (1975) Occult spinal dysraphism: a series of 73 cases. Pediatrics 55:826–835

Arber S, Han B, Mendelsohn M, Smith M, Jessell TM, Sockanathan S (1999) Requirement for the homeobox gene Hb9 in the consolidation of motor neuron identity. Neuron 23: 659–674

Bellomonte D, Di Bernardo M, Russo R, Caronia G, Spinelli G (1998) Highly restricted expression at the ectoderm-endoderm boundary of *PIHbox 9*, a sea urchin homeobox gene related to the human *HB9* gene. Mech Dev 74:185–188

Belloni E, Martucciello G, Verderio D, Ponti E, Seri M, Jasonni

V, Torre M, et al (2000) Involvement of the *HLXB9* homeobox gene in Currarino syndrome. Am J Hum Genet 66: 312–319

Bullen PJ, Robson SC, Strachan T (1998) Human post-implantation embryo collection: medical and surgical techniques. Early Hum Dev 51:213–221

Cavero Vargas E, Plauchu H, Rebaud A, Claris O, Chappuis JP, Mellier G, Salle B (1992) Anomalies du sacrum et deficit de fermeture du tube neurale: manifestations differentes d'une meme maladie genetique? Pediatrie 47:273–277

Currarino G, Coln D, Votteler T (1981) Triad of anorectal, sacral, and presacral anomalies. Am J Roentgenol 137: 395–398

Dattani M T, Martinez-Barbera J, Thomas PQ, Brickman JM, Gupta R, Martensson I, Toresson H, et al (1998) Mutations in the homeobox gene *HESX1/Hesx1* associated with septo-optic dysplasia in human and mouse. Nat Genet 19:125–133

Di Rocco G, Mavilio F, Zappavigna V (1997) Functional dissection of a transcriptionally active, target-specific Hox-Pbx complex. EMBO J 16:3644–3654

Fougerousse F, Bullen PJ, Herasse M, Lindsay S, Richard I, Wilson D, Suel L, et al (2000) Human-mouse differences in the embryonic expression patterns of developmental control genes and disease genes. Hum Mol Genet 9:165–173

Gaskill SJ, Marlin AE (1996) The Currarino triad: its importance in pediatric neurosurgery. Pediatr Neurosurg 25: 143–146

Gehring WJ, Qian YQ, Billeter M, Furukubo-Tokunaga K, Schier AF, Resendez-Perez D, Affolter M, et al (1994) Homeodomain-DNA recognition. Cell 78:211–223

Hardwick RJ, Onikul E, De Silva M, Glasson MJ, Gaskin KJ (1992) Partial sacral agenesis with constipation: a report of one family. J Pediatr Child Health 28:328–330

Harrison KA, Druey KM, Deguchi Y, Tuscano JM, Kehrl JH (1994) A novel human homeobox gene distantly related to *proboscipedia* is expressed in lymphoid and pancreatic tissues. J Biol Chem 269:19968–19975

Harrison KA, Thaler J, Pfaff SL, Gu H, Kehrl JH (1999) Pancreas dorsal lobe agenesis and abnormal islets of Langerhans in Hlxb9-deficient mice. Nat Genet 23:71–75

Heus HC, Hing A, van Baren MJ, Joosse M, Breedveld GJ, Wang JC, Burgess A, et al (1999) A physical and transcriptional map of the preaxial polydactyly locus on chromosome 7q36. Genomics 57:342–351

Kalter H (1993) Case reports of malformations associated with maternal diabetes: history and critique. Clin Genet 43: 174–179

Kedinger M (1994) Growth and development of intestinal mucosa. In: Campbell FC (ed) Small bowel enterocyte culture and transplantation. R. G. Landes, Austin, TX, pp 1–31

Kissinger CR, Liu B, Martin-Blanco E, Kornberg TB, Pabo CO (1990) Crystal structure of an engrailed homeodomain-DNA complex at 2.8 A resolution: a framework for understanding homeodomain-DNA interactions. Cell 63:579–590

Klein RM (1989) Small intestinal cell proliferation during development. In: Lebenthal EE (ed) Human gastrointestinal development. Raven, New York, pp 367–390

Li H, Arber S, Jessell TM, Edlund H (1999) Selective agenesis of the dorsal pancreas in mice lacking homeobox gene *Hlxb9*. Nat Genet 23:67–70

Lindsay S, Lako M, Bullen P, Rankin J, Strachan T (1997) Expression of *WNT* genes in post-implantation human embryos. In Strachan T, Lindsay S and Wilson DI (eds) Molecular genetics in early human development. BIOS, Oxford, pp 193–212

Lynch SA, Bond PM, Copp AJ, Kirwan WO, Nour S, Balling R, Mariman E, et al (1995) A gene for autosomal dominant sacral agenesis maps to the holoprosencephaly region at 7q36. Nat Genet 11:93–95

Mclone D, Dias M (1994*a*) Normal and abnormal early development of the nervous system. In: Cheek R (ed) Paediatric neurosurgery: surgery of the developing nervous system. 3d ed. Saunders, Philadelphia, pp 3–38

Mclone D, Dias M (1994*b*) Normal and abnormal early development of the spine. In Cheek R (ed) Paediatric neurosurgery: surgery of the developing nervous system, 3d ed. Saunders, Philadelphia, pp 40–50

Ming JE, Muenke M (1998) Holoprosencephaly: from Homer to hedgehog. Clin Genet 53:155–163

Morichon-Delvallez N, Delezoide AL, Vekemans M (1993) Holoprosencephaly and sacral agenesis in a fetus with a terminal deletion 7q36-7qter. J Med Genet 30:521–524

O'Rahilly R, Muller F (1987) Developmental stages in human embryos. Carnegie Institute, Washington

Pang D (1993) Sacral agenesis and caudal spinal cord malformations. Neurosurgery 32:755–778

Pfaff SL, Mendelsohn M, Stewart C L, Edlund T, Jessell TM (1996) Requirement for LIM homeobox gene *Isl1* in motor neuron generation reveals a motor neuron-dependent step in interneuron differentiation. Cell 84:309–320

Riggs AC, Tanizawa Y, Aoki M, Wasson J, Ferrer J, Rabin DU, Vaxillaire M, et al (1995). Characterization of the LIM/homeodomain gene islet-1 and single nucleotide screening in NIDDM. Diabetes 44:689–694

Ross AJ, Ruiz-Perez V, Wang Y, Hagan DM, Scherer S, Lynch SA, Lindsay S, et al (1998) A homeobox gene, *HLXB9*, is the major locus for dominantly inherited sacral agenesis. Nat Genet 20:358–361

Saha MS, Miles RR, Grainger RM (1997) Dorsal-ventral patterning during neural induction in Xenopus: assessment of spinal cord regionalization with *xHB9*, a marker for the motor neuron region. Dev Biol 187:209–223

Savage NM, Maclachlan NA, Joyce CA, Moore IE, Crolla JA (1997) Isolated sacral agenesis in a fetus monosomic for 7q36.1-qter. J Med Genet 34:866–868

Swaroop A, Wang Q, Wu W, Cook J, Coats C, Xu S, Chen S, et al (1999) Leber congenital amaurosis caused by a homozygous mutation (R90W) in the homeodomain of the retinal transcription factor CRX: direct evidence for the involvement of CRX in the development of photoreceptor function. Hum Mol Genet 8:299–305

Tanabe Y, William C, Jessell TM (1998) Specification of motor neuron identity by the *MNR2* homeodomain protein. Cell 95:67–80

Thaler J, Harrision K, Sharma K, Lettieri K, Kehrl J, Pfaff SL (1999) Active supression of interneuron programs within developing motor neurons revealed by analysis of homeodomain Factor Hb9. Neuron 23:675–687

Vargas FR, Roessler E, Gaudenz K, Belloni E, Whitehead AS,

Kirke PN, Mills JL, et al (1998) Analysis of the human sonic hedgehog coding and promoter regions in sacral agenesis, triphalangeal thumb, and mirror polydactyly. Hum Genet 102:387–392

Villa A, Santagata S, Bozzi F, Giliani S, Frattini A, Imberti L, Gatta LB, et al (1998) Partial V(D)J recombination activity leads to Omenn syndrome. Cell 93:885–896

Yamaguchi TP, Bradley A, McMahon AP, Jones S (1999) A Wnt5a pathway underlies outgrowth of multiple structures in the vertebrate embryo. Development 126:1211–1223